Can Cluster Structure Affect Kinetic Method Measurements? The Curious Case of Glutamic Acid's Gas-Phase Acidity

Francoise Fournier,[a] Carlos Afonso,[a] Adelaide E. Fagin,[c] Scott Gronert,[b,c] and Jean-Claude Tabet[a]

[a] Université Pierre et Marie Curie-Paris6, UMR 7613 Synthèse, Structure et Fonction de Molécules Bioactives, Paris, France
[b] Department of Chemistry, Virginia Commonwealth University, Richmond, Virginia, USA
[c] Department of Chemistry and Biochemistry, San Francisco State University, San Francisco, California, USA

The gas-phase acidities of aspartic, glutamic, and 2-aminoadipic acid have been determined by the kinetic method in a triple-quadrupole instrument. Although aspartic acid behaves in the conventional way and gives a ΔH_{acid} value of 1340 kJ mol^{-1}, glutamic and 2-aminoadipic acids give kinetic method plots with two distinct slopes. This leads to ΔH_{acid} values of 1350 and 1366 kJ mol^{-1} for glutamic acid, and 1355 and 1369 kJ mol^{-1} for 2-aminoadipic acid. The value for aspartic acid and the low collision energy value for glutamic acid are consistent with recent measurements by Poutsma and co-workers in a quadrupole ion trap. The experiments are supported by calculations at the G3(MP2) and OLYP/aug-cc-pVTZ levels. Computational studies of model clusters of the amino acids with trifluoroacetate suggest there are distinct preferences. Glutamic and 2-aminoadipic acid prefer clusters where the amino acid adopts a zwitterion-like structure whereas aspartic acid prefers to adopt a conventional (canonic) structure in its clusters. This result along with the computed stabilities of zwitterion-like conformations of the deprotonated amino acids leads to the following explanation for the presence of two slopes in the kinetic method plots. At low collision energies, the deprotonated amino acid dissociates from the cluster, with rearrangement if necessary, to give its preferred conformation, but at high collision energies, the deprotonated amino acid directly dissociates in the conformation preferred in the cluster. For glutamic and 2-aminoadipic acids, this is a zwitterion-like structure that is about 20 kJ mol^{-1} less stable than the global minimum. (J Am Soc Mass Spectrom 2008, 19, 1887–1896) © 2008 Published by Elsevier Inc. on behalf of American Society for Mass Spectrometry

The kinetic method has been used widely to measure neutral thermodynamic properties in the gas-phase, but questions still remain about the validity of some of its basic assumptions, which were initially developed around the study of monofunctional compounds and reference acids/bases whose structures are closely related to the analyte [1–3]. A key assumption is that in the dissociation transition-state, the components of the heterodimer cluster used in the kinetic method must have adopted structures that resemble those of the ultimate, separated products (i.e., no reverse activation energy in the process). One must also assume that the competitive decomposition pathways of interest in the kinetic method are independent of the initial structure of the dimeric cluster, which may depend on how it was formed in the ionization process. In addition, attempts to extract the relative standard enthalpy and entropy variations of the products also require that the ensemble of the competing transition states provides a reasonable representation of the Boltzman distribution of the separated products [4]. Finally, it is generally assumed that values from the kinetic method are relevant to a process occurring at 298 K (i.e., the clusters dissociate to the preferred conformations of the products at 298 K).

The general success of the kinetic method suggests that these assumptions are valid enough to provide reasonable accuracy in a variety of systems and that some level of natural selection in the formation of the charged heterodimer clusters limits them to fairly representative structures. However, there clearly must be many situations where the cluster components do not adopt their preferred ensemble of structures in the dissociation transition-state. In the present study, we present a clear example of the breakdown of the kinetic method in its application to multifunctional compounds using reference acids/bases that differ significantly from the structures of the analytes. In the amino acid

Address reprint requests to Dr. S. Gronert, Department of Chemistry, Virginia Commonwealth University, 1001 West Main Street, Richmond, Virginia 23284, USA. E-mail: sgronert@vcu.edu

1044-0305/08/$32.00
doi:10.1016/j.jasms.2008.07.022

Published online August 7, 2008
Received May 19, 2008
Revised July 25, 2008
Accepted July 26, 2008

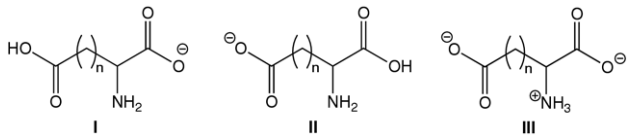

Scheme 1

systems employed in this study (aspartic, glutamic, and 2-aminoadipic acids), it will be shown that the formation of the heterodimer clusters can cause a deprotonated amino acid to adopt a zwitterionic form rather than a canonic structure. It has been noted in the past that solvation and metal complexation is capable of shifting amino acids to zwitterionic structures [5–7]. Apparently under certain collision activation conditions, the nature of the cluster (zwitterionic versus canonic) can affect the observed branching ratios in the dissociation processes and thereby alter the acidity predicted by the kinetic method analysis.

The proton affinities of amino acids have been extensively investigated, [8–11] but there have been only a few reports on their gas-phase acidities (GA, $\Delta G°_{acid}$) and acid enthalpies ($\Delta H°_{acid}$) [12]. The acidic amino acids, aspartic and glutamic acid, are interesting systems for gas-phase acidity measurements because they can adopt a variety of ionic structures in their deprotonated forms (Scheme **1**, Scheme **2**). Until very recently, no experimental gas-phase acidity values were available for them [13, 14]. However while we were completing this study, Poutsma and co-workers [15] reported values for these amino acids from kinetic method experiments in a quadrupole ion trap [$\Delta H°_{acid}$ = (1345 ± 14) kJ mol^{-1} and (1348 ± 21) kJ mol^{-1} for Asp and Glu, respectively]. In addition, Cassady and co-workers [16] have obtained gas-phase acidity values by bracketing experiments in an ICR [ΔG^0_T = (1319 ± 14) kJ mol^{-1} and (1331 ± 15) kJ mol^{-1} for Asp and Glu, respectively]. These values are in good accord with DFT and *ab initio* calculations from the two research groups. Our kinetic method studies differ from those completed by Poutsma and co-workers in that we have used a triple quadrupole instrument and accessed much higher collision energies. The data indicate that there are two distinct modes of dissociation for glutamic acid, depending on the magnitude of the collision energy. This effect leads to two sets of acidity values for glutamic acid. In contrast, aspartic acid behaves in a conventional way in the kinetic method experiments. Here we will show that the difference in behavior potentially can be traced to the ionic structure of the cluster used in the kinetic method experiments.

Experimental

All experiments were carried out on a triple quadrupole (Quattro, Micromass, Manchester, UK) instrument equipped with an electrospray source operated in the negative ion mode. Argon was used as collision gas with a pressure of 5 × 10^{-5} mbar. All the recorded spectra were the average of 150 microscans to obtain a good ion abundance statistics. All samples were purchased from Sigma-Aldrich Chemicals (St. Louis, MO) and used without further purification. The proton-bound dimers were prepared by the direct infusion (400 μL h^{-1}) of a 1:1 mixture of an amino acid and an acidic reference (100 μM in MeOH). The cone voltage was set to 30 V in order avoid in-source decomposition of the dimeric species.

Kinetic Method

In this work, the extended kinetic method [17] was used using the "statistical" approach as proposed by Armentrout [18]. All the experimental measurements were provided following this approach. However, for an easier discussion within the manuscript, the reported curves corresponded to the "alternative" [18] treatment that was almost as accurate as the "statistical" but was more intuitive. In addition, in the case of glutamic acid, the three methods (the original extended, alternative, and statistical) were used for comparison. In practice, both alternative and statistical approach gave the same results although a better error estimation was obtained with the latter. The different methods were described extensively in their original papers and are only summarized here.

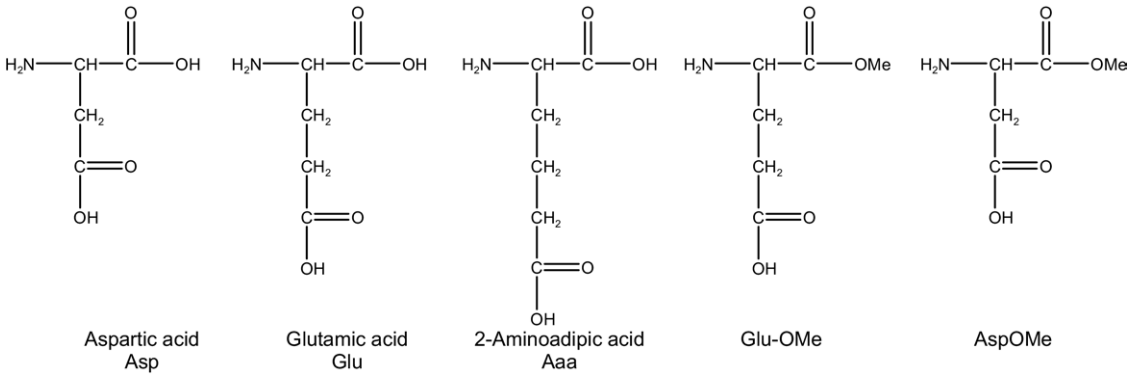

Scheme 2

For each studied amino acid (A_0) a series of references (A_i) were chosen based on the consideration that they were monofunctional and that the decompositions of the corresponding dimer $[A_0+A_i\text{-}H]^-$ led to the observation of both the expected competitive product ions $[A_0\text{-}H]^-$ and $[A_i\text{-}H]^-$. For each amino acid at least four references were used. These experiments were repeated at various collision energies varying from 10 to 60 eV in the laboratory frame to change significantly the effective temperature.

The alternative method was based on eq 1. A series of curves $\ln(k_i/k_0)$ (that were considered to be equal to the corresponding product ion abundance ratio) were plotted as a function of the $\Delta H°_{acid}$ values of the references for each collisional activation condition.

$$\ln\frac{k_i}{k_0} = \frac{GA^{app}_{T_{eff}}(A_0)}{RT_{eff}} - \frac{\Delta H^{\circ}_{acid}(A_i)}{RT_{eff}} \quad (1)$$

with

$$GA^{app}_{T_{eff}}(A_0) = \Delta H^{\circ}_{acid}(A_0) - T_{eff}\Delta\Delta S^{\circ}_{acid}(A_i, A_0)\ [19]. \quad (2)$$

The x-intercept of these curves was the apparent gas-phase acidity of the unknown, $GA^{app}_{T_{eff}}(A_0)$ and the slope is $-1/RT_{eff}$. From these data, a second curve $GA^{app}_{T_{eff}}(A_0)$ as a function of T_{eff} was plotted. From eq 2, it can be observed that the y-intercept of this curve is $\Delta H°_{acid}(A_0)$ and the slope is $-\Delta\Delta S°(A_0,A_i)$.

For the "statistical" approach, the first plot is $\ln(k_i/k_0)$ versus $\Delta H°_{acid}(A_0)$-$\Delta H°_{acid}(A_i)_{avg}$. From eq 3, it can be seen that the slope corresponds to $-1/RT_{eff}$ and the y-intercept is $[GA^{app}_{T_{eff}}(A_0) - \Delta H^{\circ}(A_i)_{avg}]/RT_{eff}$. From these data, the curve $[GA^{app}_{T_{eff}}(A_0) - \Delta H^{\circ}(A_i)_{avg}]/RT_{eff}$ as a function of $1/RT_{eff}$ was plotted leading in principle to a straight line. According to eq 4, the slope of this line was $\Delta H°_{acid}(A_0)$-$\Delta H°_{acid}(A_i)_{avg}$ and its y-intercept was $-\Delta\Delta S°/R$.

$$\ln\frac{k_i}{k_0} = \frac{GA^{app}_{T\,eff}(A_0) - \Delta H^{\circ}(A_i)_{avg}}{RT_{eff}} - \frac{\Delta H^{\circ}_{acid}(A_i) - \Delta H^{\circ}(A_i)_{avg}}{RT_{eff}} \quad (3)$$

From Equation 2

$$\frac{GA^{app}_{T\,eff}(A_0) - \Delta H^{\circ}_{acid}(A_i)_{avg}}{RT_{eff}} = \frac{\Delta H^{\circ}_{acid}(A_i) - \Delta H^{\circ}(A_i)_{avg}}{RT_{eff}} - \frac{\Delta\Delta S^{\circ}(A_0, A_i)}{R} \quad (4)$$

Experimental errors (standard deviations) were calculated from experimental deviations and taking into account uncertainties of the reference acidity values based on the Armentrout treatment [18]. More recently, Armentrout considered that errors in the $\Delta H°$ values are about ± 4 to ± 12 kJ mol^{-1} (± 9 to ± 30 J mol^{-1} K^{-1} for activation entropy differences), whereas Drahos, Vekey, and others have suggested an estimated error of ± 5 kJ mol^{-1} [± 10 J mol^{-1} K^{-1} for $\Delta\Delta S°(A_0,A_i)$] [4, 20].

Computational

Each of the species in this study presented a difficult problem in terms of computational method and conformational space. Standard ab initio methods such as HF and MP2 calculations typically gave poor results for the absolute acidities of carboxylic acids. Common DFT approaches such as B3LYP also had a difficult time with the absolute acidities of these species. For this study, we decided to use an alternative DFT approach, OLYP, to survey the potential energy surface and identify the lowest energy conformations of each species. It was chosen because it gave good performance with carboxylic acids. For example, OLYP/aug-cc-pVTZ//B3LYP/6-31 + G(d,p) calculations gave a ΔH_{acid} value of 1453 kJ mol^{-1} for acetic acid (experimental = 1456 kJ mol^{-1}). In contrast, B3LYP and MP2 calculations gave values of 1448 and 1443 kJ mol^{-1} with the same basis set and geometry. We have adopted multiple strategies for identifying the best conformer of each species and determining the absolute gas-phase acidities of the amino acids. For all species, the conformational search utility in Spartan02 was used to identify the 100 lowest energy conformations at the PM3 semiempirical level. Only conformations within 125 kJ mol^{-1} of the global minimum were pursued. As a result, less than 100 conformations were considered for several of the species. The best conformations from the PM3 searches were subjected to single point calculations at the OLYP/6-31 + G(d) level. The best 30 from these calculations were then subjected to optimizations and frequency analysis at the OLYP/6-31 + G(d) level followed by single points at the OLYP/aug-cc-pVTZ level. The best conformations at this level (10–30 conformations) were subjected to G3(MP2) calculations. In some cases, a second set of searches was included. This involved identifying up to the best 250 conformations at the PM3 level, selecting the best 50 of these at the B3LYP/6-31 + G*//PM3 level, and subjecting those to G3MP2 calculations. The acidities were reported at the G3(MP2) level and included thermal enthalpy corrections scaled by 0.9135. The best conformer was determined on the basis of the lowest computed free-energy at 298 K so in a few cases, the species that was used in the calculation did not have the lowest computed enthalpy. The logic of this decision is that the experimental mixture of conformers is determined on the basis of free energies, not enthalpies. The clusters in the study were too large for the G3(MP2) calculations and their energies were reported at the OLYP/aug-cc-pVTZ//OLYP/6-31 + G(d) level with unscaled thermal enthalpy corrections. The PM3 surveys were completed with Spartan02 [21] and the other calculations

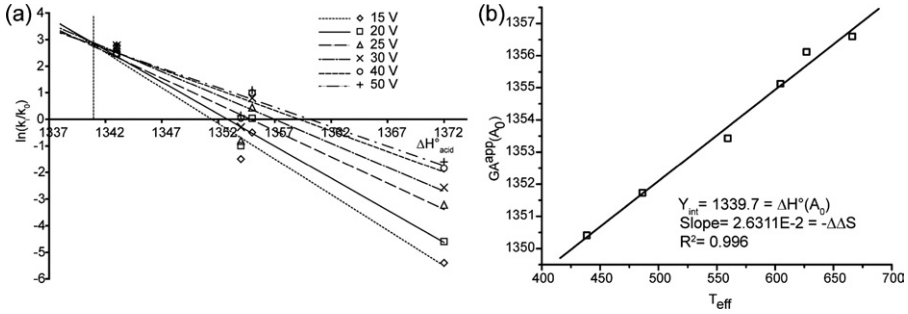

Figure 1. Kinetic method plots for aspartic acid (**a**) $\ln(k_i/k_0)$ versus $\Delta H°(A_i)$ (**b**) $GA^{app}(A_0)$ versus T_{eff} (alternative treatment).

with Gaussian03 [22]. Details of the calculations are found in Supplementary Material, which is available in the online version at doi:10.1016/j.jasms.2008.07.022.

Results

Aspartic Acid

The kinetic method plots for aspartic acid are given in Figure 1. The plots span effective temperatures from about 440 to 666 K. As reference acids, a series of simple acids and phenols were used (Table 1). The final plot (Figure 1b) is reasonably linear and indicates a $\Delta H°_{acid}$ value of 1340 kJ mol^{-1} with a proton transfer entropy variation of $\Delta\Delta S°_{acid} = -27$ J mol^{-1} K^{-1} related to the acidic references (Table 2). It can be seen that all the lines of the first plot cross nicely in a single point (Figure 1a). This point has been called the pseudo-isoequilibrium by Armentrout and the corresponding abscissa gives the $\Delta H°_{acid}$ [4]. These values are in good accord with those obtained by Poutsma in a quadrupole ion trap [$\Delta H°_{acid} = (1345 \pm 14)$ kJ mol^{-1} and $\Delta\Delta S°_{acid} = (-14 \pm 14)$ J mol^{-1} K^{-1}] [15]. It should be noted that the proton transfer entropy values cannot be directly compared because different references were used in the experiments; this is also true for the other amino acids in this study. It is more difficult to make comparisons to the free-energies reported by Cassady and co-workers [16]; however both datasets indicate that the gas-phase acidity of aspartic acid is close to that of trifluoroacetic acid.

Using the structures in Figure 2a and b, we have computed a $\Delta H°_{acid}$ value of 1347 kJ mol^{-1} for aspartic acid. This value is reasonably close to the experimental values and those computed by Poutsma [15] as well as Cassady et al. [16]. It should be noted that our structures are significantly different. DFT approaches used by the other groups to identify the most stable conformer tend to favor canonic amino acid structures where the α-carboxylic acid forms a hydrogen-bond with the amino group. In contrast, G3MP2 generally favors carboxyl groups with internal hydrogen bonds (syn conformations). The effect on the computed energies is not large and leads to differences of 1–4 kJ mol^{-1} in the acidities. We also computed a $\Delta H°_{acid}$ value for the formation of a zwitterionic-like species, Figure 2c. It is not a true zwitterion in that the nitrogen has only a strong hydrogen-bonding interaction with a third proton rather than a full bond, but it exhibits the heavy atom topology of a zwitterion. No true zwitterionic species were found with the computational methods used in this study, indicating a small or nonexistent

Table 1. Acidic references

A_i	$\Delta H°_{acid}(A_i)$ kJ.mol^{-1}	Corresponding unknown (A_0)
CH_3SO_3H	1343 ± 9.2[a]	Asp
Pentafluorobenzoic acid	1354 ± 8.8[a]	Asp, Aaa[c]
CF_3COOH	1355 ± 12.0[a]	Asp, Glu
COOH-COOH	1356 ± 8.0[b]	Glu
4-Nitrophenol	1372 ± 8.8[a]	Asp, Glu, Aaa[c]
4-Nitrobenzoic acid	1373 ± 9.2[a]	Glu, Aaa[c]
3-Methyl-4-nitrophenol	1380 ± 8.8[a]	Aaa[c]
3-Nitrophenol	1399 ± 8.8[a]	AspOMe
3-Cyanophenol	1405 ± 8.8[a]	AspOMe
4-Trifluoromethylphenol	1410 ± 8.8[a]	AspOMe
2,6-Dimethylbenzoic acid	1416 ± 8.8[a]	GluOMe
2,3-Dimethylbenzoic acid	1419 ± 8.8[a]	AspOMe, GluOMe
4-Methoxybenzoic acid	1426 ± 8.8[a]	AspOMe, GluOMe
4-Methylbenzoic acid	1427 ± 8.8[a]	AspOMe, GluOMe
3-Chlorophenol	1433 ± 21[a]	GluOMe
4-Chlorophenol	1436 ± 8.8[a]	GluOMe

[a]From NIST webbook [27].
[b]From reference [23].
[c]2-Aminoadipic acid.

Table 2. Experimental results using the extended kinetic method following the "statistic" approach[a]

A_i	CE (eV)	T_{eff} range (K)	$\Delta H°_{acid}(A_i)$ kJ mol^{-1}	$\Delta\Delta S°$ J mol K^{-1}
Glu	10–35	319–413	1350 ± 6	−42 ± 4
	35–60	413–550	1366 ± 5	−4 ± 2
Asp	10–60	440–666	1340 ± 5	−27 ± 1
Aaa[b]	10–40	534–922	1355 ± 5	−21 ± 1
	40–60	922–1011	1368 ± 6	−6 ± 2
GluOMe	10–45	406–599	1420 ± 4	−14 ± 1
AspOMe	10–60	708–3767	1413 ± 4	0 ± 1

[a]The uncertainties are derived from the kinetic method plots. The absolute uncertainties in ΔH° are much larger because the uncertainties of the reference compounds in Table 1 must be incorporated.
[b]2-Aminoadipic acid.

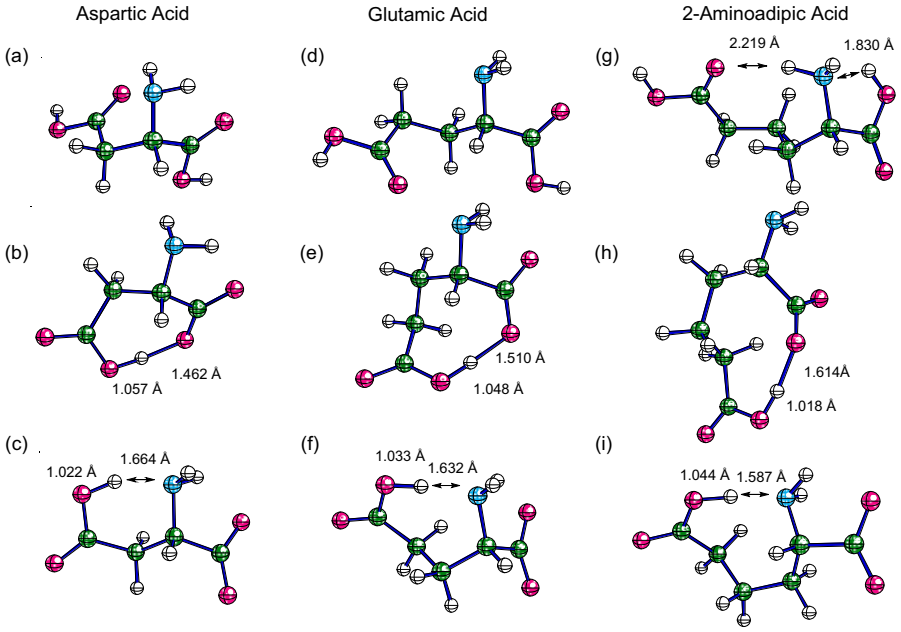

Figure 2. Low-energy structures of (**a**) aspartic acid, and (**b**) deprotonated aspartic acid, (**c**) zwitterion-like deprotonated aspartic acid, (**d**) glutamic acid, (**e**) deprotonated glutamic acid, (**f**) zwitterion-like deprotonated glutamic acid, (**g**) 2-aminoadipic acid, (**h**) deprotonated 2-aminoadipic acid, and (**i**) zwitterion-like deprotonated 2-aminoadipic acid. Calculations at the MP2/6-31 + G(d) level.

barrier to shuttling the proton between the amino and carboxylic acid groups. The zwitterion-like structure in Figure 2c is disfavored by 23 kJ mol^{-1} and yields a $\Delta H°_{acid}$ value of 1370 kJ mol^{-1}. Also, the cyclic, internally hydrogen-bonded structure in Figure 2b is much more stable (>60 kJ mol^{-1}) than any acyclic (unfolded) structures lacking an internal hydrogen bond to the un-ionized carboxylic acid. These kinetic method data suggest that throughout the energy regime, dissociation leads to deprotonated aspartic acid in a structure close to that shown in Figure 2b.

Glutamic Acid

The kinetic plots for glutamic acid (Figure 3) present a different picture and two distinct slopes are seen. The first spans the effective temperature region from 319 to 413 K and the second from 413 to 550 K (Figure 3b). The plots lead to two sets of estimated thermochemical values with $\Delta H°_{acid}$ values of 1350 kJ mol^{-1} and 1366 kJ mol^{-1}, and relative proton transfer standard entropies of −42 J mol^{-1} K^{-1} and −4 J mol^{-1} K^{-1} (Table 2). Interestingly, these two slopes are observed in both *alternative* (Figure 3b) and *statistic* (Figure 3c) method plots but not in the conventional extended method plot (Figure 3d). This is an excellent example of how the conventional extended plot method can hide rather large deviations from linearity in the kinetic method analysis and can give flawed data with no warning. It should be noted that in the higher effective temperature range, dissociation of the clusters gives data that indicate that glutamic acid is less acidic (i.e., higher $\Delta H°_{acid}$). In contrast, Poutsma found a single slope in their kinetic plot corresponding to a $\Delta H°_{acid}$ value of 1348 ± 21 kJ mol^{-1} with a relative proton transfer entropy variation of −20 ± 41 J mol^{-1} K^{-1} in the ion trap using other reference compounds [15]. For comparison, effective temperatures in the ion trap dissociations are expected to be in the range 300 to 400 K. This corresponds to the effective temperature range of the first slope 319–413 of our study. Taking into account the uncertainties of the measurements, there is good overlap between our low effective temperature values and those obtained by Poutsma [15]. The bracketing experiments by Cassady et al. [16] also suggest a $\Delta H°_{acid}$ value in this general range.

We have computed a $\Delta H°_{acid}$ value of 1346 kJ mol^{-1} for glutamic acid based on the structures in Figure 2d and e. Again, this value is close to the computational values reported by Poutsma group and the Cassady group despite some differences in the structures used for the calculation. Although there is some scatter in the kinetic method data from the two laboratories, the results suggest that at low collision energies, deprotonated glutamic acid is expelled from the cluster in a cyclic form similar to that shown in Figure 2e. The key question is what is happening at the higher collision energies. The more favorable entropy and higher $\Delta H°_{acid}$ value associated with the second slope could suggest that an acyclic form of the deprotonated glutamic acid is being formed. Calculations on a model, linear structure discount this explanation. Its computed

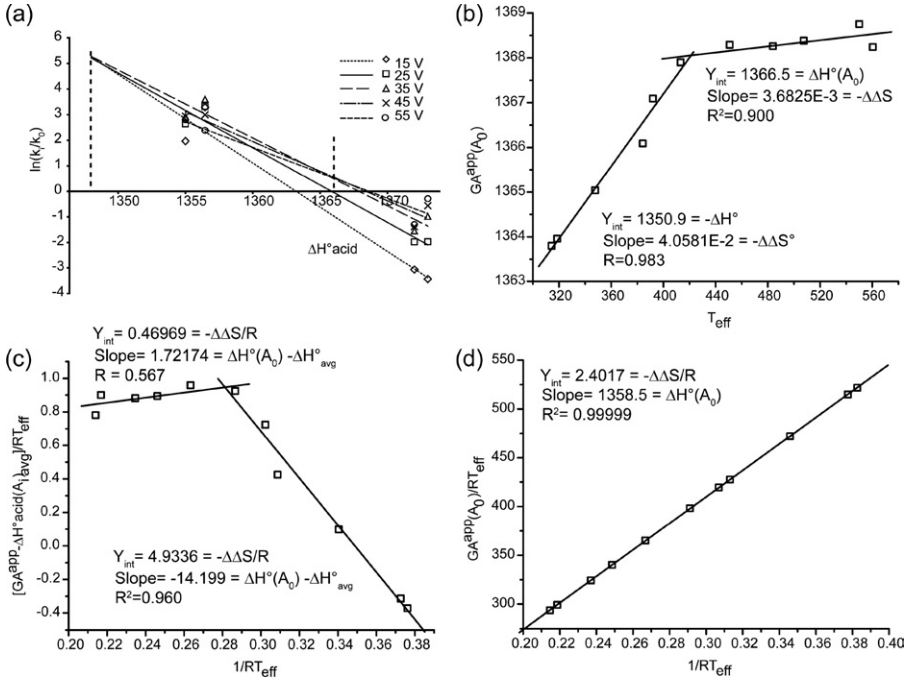

Figure 3. Kinetic method plots for glutamic acid (**a**) $\ln(k_i/k_0)$ versus $\Delta H°(A_i)$ (**b**) $GA^{app}(A_0)$ versus $T_{eff)}$ (alternative treatment) (**c**) $[GA^{app}(A_0)-\Delta H°_{avg}]/RT_{eff}$ versus $1/RT_{eff}$ (statistical treatment) (**d**) $GA^{app}(A_0)/RT_{eff}$ versus $1/RT_{eff}$ (original extended method).

$\Delta H°_{acid}$ is nearly 1412 kJ mol^{-1}, far higher than the value suggested by the second slope. A second option would be the formation of deprotonated glutamic acid in its zwitterionic form. Again, we could not locate a true zwitterion on the potential surface, but the best structure with a zwitterion-like topology is shown in Figure 2f. This species yields a $\Delta H°_{acid}$ value of 1365 kJ mol^{-1}. It is 20 kJ mol^{-1} less stable than the structure in Figure 2e. This difference in stability is close to the difference in kinetic method plot slopes, which yields 16 kJ mol^{-1}. This situation offers the intriguing possibility that the zwitterionic-like form is being produced in the high-energy fragmentations. To further investigate this possibility, experiments were also completed on the next larger species in this homologous series, 2-aminoadipic acid.

2-Aminoadipic Acid

The kinetic method and structural plots for 2-aminoadipic acid (Aaa) are presented in Figure 4a. Again, two slopes are seen in the kinetic method plot. They lead to $\Delta H°_{acid}$ values of 1355 kJ mol^{-1} and 1368 kJ mol^{-1} with relative proton transfer entropy variations of -21 J mol^{-1} K^{-1} and -6 J mol^{-1} K^{-1}. In this case, the computed value for 2-aminoadipic acid, 1362 kJ mol^{-1} (folded form, Figure 2h), is between the experimental values for the low and high effective temperature ranges (Table 3). An unfolded conformation of the anion was also calculated and its formation would lead to a $\Delta H°_{acid}$ value of 1424 kJ mol^{-1}, far higher than either of the experimental values (Table 2). The zwitterionic-like form of this ion is calculated to be 21 kJ mol^{-1} less stable than the form shown in Figure 2h and would lead to a $\Delta H°_{acid}$ value of 1383 kJ mol^{-1}. Again, this difference in stability (21 kJ mol^{-1}) is fairly close to the difference observed in the slopes (i.e., 13 kJ mol^{-1}) from the kinetic method plot (although the absolute values differ significantly). The discrepancy here may in part be driven by the fact that the second slope for 2-aminoadipic acid could only be observed over a fairly narrow range of effective temperatures and therefore has a significant uncertainty in the value.

Methyl Esters of Aspartic and Glutamic Acid

To confirm that the side-chain carboxylic acids were involved in the observed behavior, the kinetic method was applied to the acidities of the side-chain methyl esters of aspartic and glutamic acid. The kinetic method plots give a single slope in each case and point to $\Delta H°_{acid}$ values of 1413 kJ mol^{-1} for AspOMe (Figure 4b) and 1420 kJ mol^{-1} for GluOMe (Figure 4c), respectively. The computed values are 1413 and 1424 kJ mol^{-1}, respectively (Table 3). These results confirm that hydrogen bonding to the side-chain carboxylic acid groups plays an important role in determining the experimental acidities and suggest that the difference in behavior between aspartic and glutamic acid in the kinetic method experiments is related to this hydrogen bonding. Interestingly, the effective temperatures obtained for AspOMe rise to very high values (3800 K). Such very high T_{eff} is rarely observed, and usually has been obtained for the dissociation of covalently bound aromatic compounds or of inorganic salts.

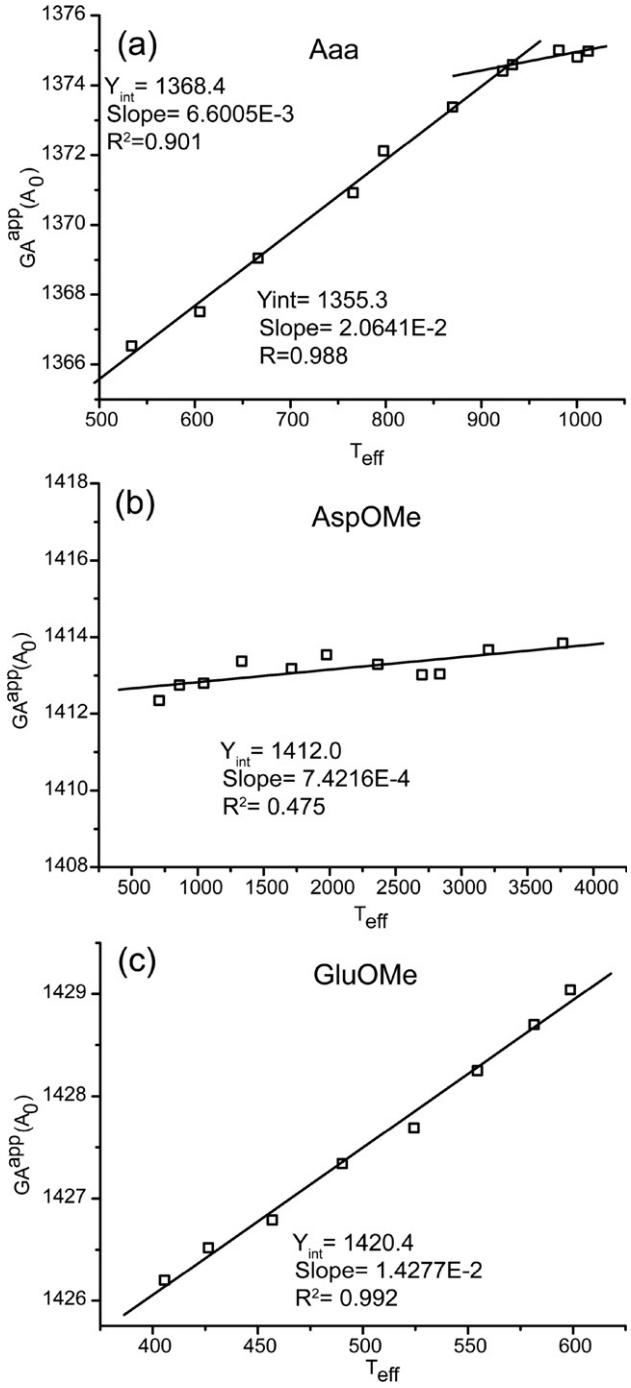

Figure 4. Curves $GA^{app}(A_0)$ versus $T_{eff)}$ (alternative treatment) for (**a**) Aaa, (**b**) AspOMe and (**c**) GluOMe.

Discussion

The results point to a sharp difference in behavior in kinetic method acidities for aspartic and glutamic acid. This is surprising given the similarity of their structures. The same unusual behavior noted for glutamic acid (i.e., two slopes in the kinetic plot) is also apparent for 2-aminoadipic acid. The key to understanding the variation in the behavior has to be related to structural/energetic differences in these highly related systems. A number of potential factors are easily eliminated.

First, the $\Delta H°_{acid}$ values are very similar for all three studied compounds and in fact, are almost identical for aspartic and glutamic acid. This result limits some of the potential for experimental errors because the same reference acids were used for both the aspartic and glutamic acids. Second, all of the acids adopt similar, preferred conformations for their anions. Third, the production of an acyclic conformation of the anion is almost equally unfavorable enthalpically for the three amino acids. It is true that formation of acyclic conformations will be more favorable entropically for the larger systems, but as noted above, the large gap between the calculated stability of the unfolded forms of the anions and the observed differences in the kinetic method slopes make the formation of acyclic anions unlikely. Fourth, each of the deprotonated amino acids can adopt a zwitterionic-like form. There is some variation in the relative stabilities of the zwitterionic-like forms, but it spans only 2 kJ mol^{-1} from deprotonated aspartic acid (disfavored by 23 kJ mol^{-1}) to deprotonated aminoadipic acid (disfavored by 21 kJ mol^{-1}). Based on these factors, it is difficult to rationalize why there would be a large difference in the behavior of these amino acids in kinetic method acidity measurements. It should be noted that Kumar et al. [23] did not see this behavior in a kinetic method study of simple dicarboxylic acids, but they did not use high collision energies so a direct comparison is not possible.

In an effort to gain more information about the dissociation processes these compounds undergo during the kinetic method experiments, we have computationally modeled a sample cluster of each of the amino acids with trifluoroacetate. The same procedure that was used to identify low-energy conformations of the neutral and deprotonated amino acids was applied to the clusters. A survey of the low-energy cluster conformations pointed to two distinct types of structures. In the first, the amino acid component of the cluster adopts a conformation where the alpha and side-chain carboxylic acid groups interact directly (hydrogen-

Table 3. Computed and literature $\Delta H°_{acid}$ values[a]

Acid	Global minimum	Zwitterion	"Linear"[b]	Experimental
Asp	1347	1370	1411	1345[d]
Glu	1346	1365	1412	1348[d]
Aaa[c]	1362	1383	1424	—
AspOMe	1413			—
GluOMe	1424			—
Gly	1435			1434[d]
Acetic acid	1458			1456[e]

[a]Values in kJ mol^{-1} for forming anion in designated structure. Computations at G3(MP2) level. See text for details.
[b]Stretched conformation with no internal hydrogen bonding interactions.
[c]2-Aminoadipic acid.
[d]Data from Poutsma and co-workers [15].
[e]Data from NIST web book [27].

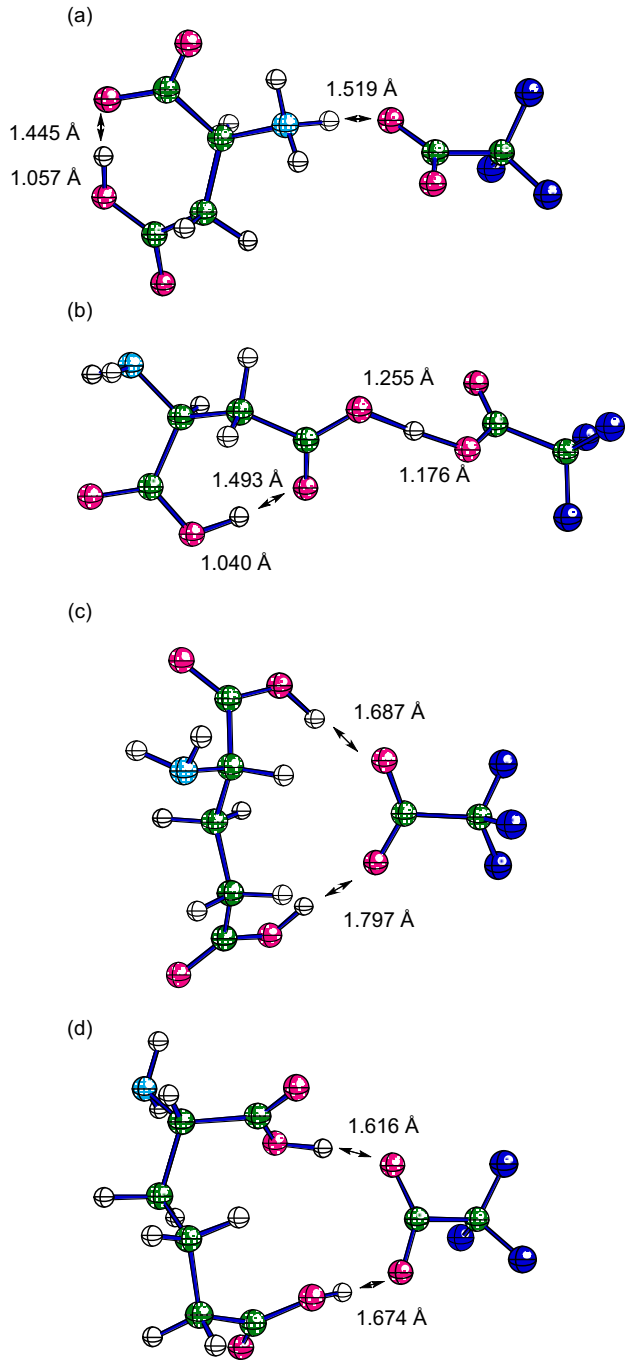

Figure 5. Low-energy, type 1 clusters of trifluoroacetate with (**a**) aspartic acid (solvated ZW/salt bridge), (**b**) aspartic acid (solvated canonic form), (**c**) glutamic acid (solvated canonic form), and (**d**) 2-aminoadipic acid (solvated canonic form). Calculations at the OLYP/6-31 + G(d) level.

bonded) or are in close proximity to each other (both hydrogen-bonding to the trifluoroacetate). In Figure 5, the most stable examples of this mode (Type 1) are shown for each of the amino acids (two distinct, but energetically similar varieties are shown for aspartic acid). It is interesting to note that in both of the low-energy aspartic acid clusters (Figure 5a and b), the amino acid component is already in a conformation similar to that preferred by the bare anion. Moreover, the proton is almost equally shared in the structure in Figure 5b, as one would expect given that aspartic and trifluoroacetic acid have similar gas-phase acidities. For glutamic acid and aminoadipic acid, such structures are not preferred and clusters where both carboxylic acids interact with the trifluoroacetate are more stable. Nonetheless, direct dissociation of any of these structures (Figure 5) to the deprotonated amino acid should lead to conformations like the preferred, internally hydrogen-bonded structures shown in Figure 2b, e, and h for the deprotonated amino acids. In the second type of cluster (Type 2), the alpha and side-chain carboxylic acid groups do not interact with each other and are separated by the amino group. The most stable examples for the three amino acids are shown in Figure 6. In each, the trifluoroacetate component interacts strongly with one

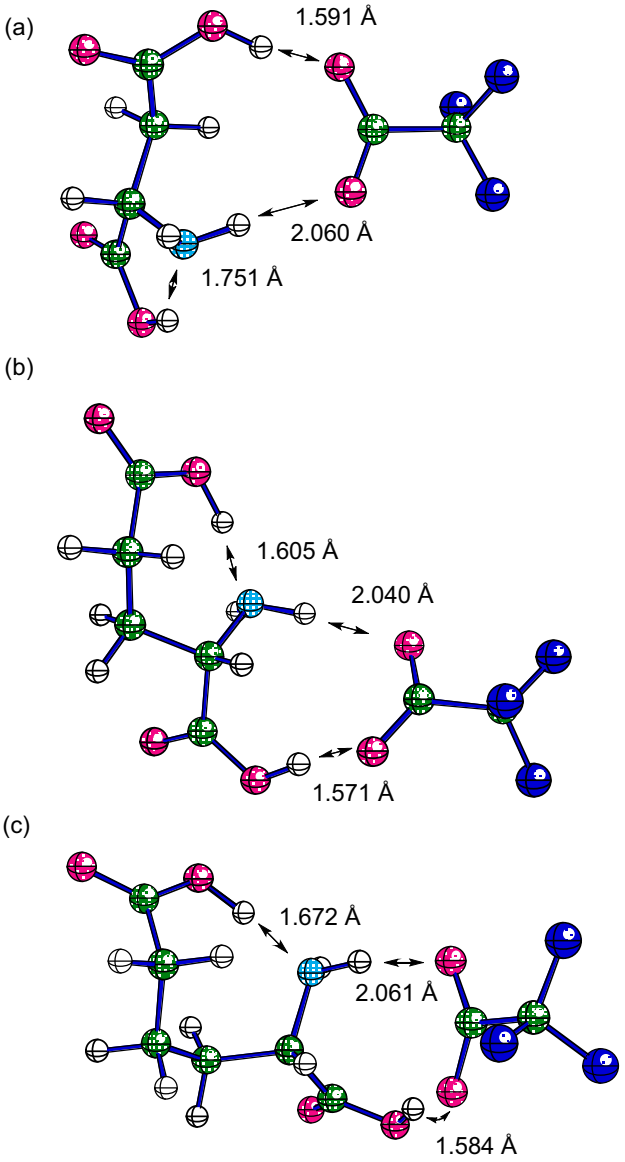

Figure 6. Low-energy, type 2 clusters of trifluoroacetate with (**a**) aspartic acid, (**b**) glutamic acid, and (**c**) 2-aminoadipic acid. Calculations at the OLYP/6-31 + G(d) level.

of the amino acid's carboxyl groups and weakly with its amine. With aspartic acid, the α-carboxylic acid group forms an internal hydrogen bond with the amino group, whereas the other amino acids prefer to use their side-chain carboxylic acid group to form this hydrogen bond. Direct dissociation of the clusters shown in Figure 6 should initially lead to structures suitable for forming the zwitterionic-like forms of the deprotonated amino acids (Figure 2c, f, and i). The interesting aspect of this survey of the clusters is that aspartic acid exhibits a clear preference for clusters of Type 1 (Figure 5) whereas glutamic and aminoadipic acids prefer Type 2 clusters (Figure 6). The binding energies of the best clusters of each type are shown in Table 3. The change in the binding preferences is significant and amounts to a swing of 14.2 kJ mol^{-1} when comparing aspartic acid to glutamic acid. The former prefers a Type 1 structure by 5.8 kJ mol^{-1} and the latter a Type 2 structure by 8.4 kJ mol^{-1} (Table 4). This difference must in part be rooted in the greater stability of zwitterion-like structures for deprotonated glutamic acid and aminoadipic acid. In any case, this difference offers a handle for rationalizing the differing behavior of the amino acids in the kinetic method experiments.

The data suggest the following scenario. At low collision energies, the negatively charged clusters are able to rearrange during the dissociation process and produce the more stable structure of the deprotonated amino acid. The structure of the cluster itself has little impact on the observed ratios. At higher collision energies, two factors may work against the rearrangements for glutamic and 2-aminoadipic acids. First, the negative activation entropy associated with the rearrangement may make the process unfavorable at higher effective temperatures, forcing the direct dissociation to the zwitterion-like structure to be more favorable in terms of activation free-energy. This is the situation assumed in the thermodynamic analysis of the kinetic plots with two slopes. Second, the dissociation may occur promptly at higher energies without a statistical reorganization of the internal energy. In other words, dissociation goes directly to structures like those preferred in the cluster despite the potential of a lower energy, rearrangement pathway on the surface. The present data do not allow one to distinguish between these two possibilities, but do indicate that one must be careful in the analysis of kinetic method dissociations at higher collision energies. This issue is not new and other authors have noticed problems in the kinetic method when a range of higher energy collisions are employed. The 1,ω-diaminoalkanes provide a good example [24, 25].

Table 4. Complexation energies with trifluoroacetate[a]

Amino acid	Type 1	Type 2
Asp	−99.1	−93.3
Glu	−96.2	−104.6
Aaa[b]	−105.8	−110.0

[a]Calculated at OLYP/aug-cc-pVTZ//OLYP/6-31+G(d) level. Values in kJ mol^{-1}.
[b]2-Aminoadipic acid.

The key problem that this study suggests is that kinetic shifts may play a role in studies using the kinetic method to evaluate thermochemistry. If the preferred structure/conformation of the analyte changes markedly in the dissociation of the kinetic method cluster, there is the definite possibility of a barrier, entropic or enthalpic, on the path to the dissociation products. Whether such a barrier affects the measurements would depend on the nature of the dissociation process. The process could involve two steps: (1) separation to give a loose orbiting complex with a reasonable lifetime followed by (2) complete separation. In this case, the kinetic barrier associated with rearrangement would likely be involved in step 1. Under low-energy, multi-collision dissociation conditions, the first step can represent a rapid, pseudo-equilibrium process and it therefore would be unaffected by the rearrangement barrier. On the other hand, if dissociation proceeds directly from the tight complex to the separated products, the kinetic barrier to rearrangement must play a role in the observed product ratio. This would be most likely under conditions where dissociation is initiated by few, high-energy collisions. This description is closely related to the transition-state switching mechanism presented by Wesdemiotis [26], except that here we propose that there is a true barrier (saddle-point) separating the tight complex from the loose complex. As noted above, we do not have appropriate data to elucidate the details of the dissociation process in these systems, but our results and the above discussion highlight the complications of extending the kinetic method approach to systems with a high degree of conformational freedom and multiple stable ionic structures.

Conclusions

When moderately high collision energies are used in the kinetic method, the assumption that the components can rearrange during the dissociation to their most stable conformation at 298 K may not be valid. In the present study, the presence of two slopes in the kinetic method plots involving glutamic and 2-aminoadipic acid suggest two different dissociation processes. The difference in acidity indicated by the two slopes is not consistent with the formation of the deprotonated amino acids in entropically favorable, linear conformations at higher effective temperatures. Instead, it correlates with the formation of the deprotonated amino acid in a zwitterion-like conformation. This conformation is preferred in clusters of glutamic and 2-aminoadipic acid with trifluoroacetate. These results suggest that at higher collision energies, deprotonated glutamic and 2-aminoadipic acid do not rearrange to their preferred conformations during the dissociation process and therefore the observed values correspond to the zwitterion-like conformation preferred in the cluster.

Overall, this work indicates that care must be taken in the interpretation of kinetic method data for species with high conformational freedom and the ability to form distinct ionic structures with barriers to rearrangement.

Acknowledgments

The authors gratefully acknowledge access to the VCU High-Performance Computing Center. They acknowledge generous support from the National Science Foundation (CHE-0716147) and from the University Pierre et Marie Curie (invited professor program). They also thank the referees for very helpful suggestions.

References

1. Cooks, R. G.; Kruger, T. L. Intrinsic Basicity. Determination Using Metastable Ions. *J. Am. Chem. Soc.* **1977,** *99,* 1279–1281.
2. McLuckey, S. A.; Cameron, D.; Cooks, R. G. Proton Affinities from Dissociations of Proton-Bound Dimers. *J. Am. Chem. Soc.* **1981,** *103,* 1313–1317.
3. Bouchoux, G.; Buisson, D. A.; Bourcier, S.; Sablier, M. Application of the Kinetic Method to Bifunctional Bases ESI Tandem Quadrupole Experiments. *Int. J. Mass Spectrom.* **2003,** *228,* 1035–1054.
4. Ervin, K. M.; Armentrout, P. B. Systematic and Random Errors in Ion Affinities and Activation Entropies from the Extended Kinetic Method. *J. Mass Spectrom.* **2004,** *39,* 1004–1015.
5. Jockusch, R. A.; Lemoff, A. S.; Williams, E. R. Effect of Metal Ion and Water Coordination on the Structure of a Gas-Phase Amino Acid. *J. Am. Chem. Soc.* **2001,** *123,* 12255–12265.
6. Julian, R. R.; Beauchamp, J. L.; Goddard, W. A. Cooperative Salt Bridge Stabilization of Gas-Phase Zwitterions in Neutral Arginine Clusters. *J. Phys. Chem. A* **2002,** *106,* 32–34.
7. Boutin, M.; Bich, C.; Afonso, C.; Fournier, F.; Tabet, J. C. Negative-Charge Driven Fragmentations for Evidencing Zwitterionic Forms from Doubly Charged Coppered Peptides. *J. Mass Spectrom.* **2007,** *42,* 25–35.
8. Meotner, M.; Hunter, E. P.; Field, F. H. Ion Thermochemistry of Low-Volatility Compounds in The Gas-Phase. 1. Intrinsic Basicities of α-Amino-Acids. *J. Am. Chem. Soc.* **1979,** *101,* 686–689.
9. Afonso, C.; Modeste, F.; Breton, P.; Fournier, F.; Tabet, J. C. Proton Affinities of the Commonly Occurring L-Amino Acids by Using Electrospray Ionization-Ion Trap Mass Spectrometry. *Eur. J. Mass Spectrom.* **2000,** *6,* 443–449.
10. Bleiholder, C.; Suhai, S.; Paizs, B. Revising the Proton Affinity Scale of the Naturally Occurring α-Amino Acids. *J. Am. Soc. Mass Spectrom.* **2006,** *17,* 1275–1281.
11. Dinadayalane, T. C.; Sastry, G. N.; Leszczynski, J. Comprehensive Theoretical Study Towards the Accurate Proton Affinity Values of Naturally Occurring Amino acids. *Int. J. Quantum Chem.* **2006,** *106,* 2920–2933.
12. Ohair, R. A. J.; Bowie, J. H.; Gronert, S. Gas-Phase Acidities of the α-Amino-Acids. *Int. J. Mass Spectrom. Ion Processes* **1992,** *117,* 23–36.
13. Afonso, C.; Alves, S.; Fournier, F.; Lesage, D.; Fagin, A. E.; Gronert, S.; Tabet, J. C. Interactions of Deprotonated Amino Acids with Cyclodextrins: The Acidity of Aspartic and Glutamic Acid. *Proceedings of the 54th ASMS Conference on Mass Spectrometry and Allied Topics*; Seattle, WA, June 2006.
14. Colyer, K. E.; Jones, C. M.; Metz, R.; Pawlow, A.; Wischow, E. D.; Poutsma, J. C. Gas Phase Acidities of the 20 Protein Amino Acids from the Extended Kinetic Method. *Proceedings of the 54th ASMS Conference on Mass Spectrometry and Allied Topics*; Seattle, WA, June 2006.
15. Jones, C. M.; Bernier, M.; Carson, E.; Colyer, K. E.; Metz, R.; Pawlow, A.; Wischow, E. D.; Webb, I.; Andriole, E. J.; Poutsma, J. C. Gas-Phase Acidities of the 20 Protein Amino Acids. *Int. J. Mass Spectrom.* **2007,** *267,* 54–62.
16. Li, Z.; Matus, M. H.; Velazquez, H. A.; Dixon, D. A.; Cassady, C. J. Gas-Phase Acidities of Aspartic Acid, Glutamic Acid, and Their Amino Acid Amides. *Int. J. Mass Spectrom.* **2007,** *265,* 213–223.
17. Cheng, X. H.; Wu, Z. C.; Fenselau, C. Collision Energy-Dependence of Proton-Bound Dimer Dissociation-Entropy Effects, Proton Affinities, and Intramolecular Hydrogen-Bonding In Protonated Peptides. *J. Am. Chem. Soc.* **1993,** *115,* 4844–4848.
18. Armentrout, P. B. Entropy Measurements and the Kinetic Method: A Statistically Meaningful Approach. *J. Am. Soc. Mass Spectrom.* **2000,** *11,* 371–379.
19. Nold, M. J.; Cerda, B. A.; Wesdemiotis, C. Proton Affinities of the N- and C-Terminal Segments Arising Upon the Dissociation of the Amide Bond in Protonated Peptides. *J. Am. Soc. Mass Spectrom.* **1999,** *10,* 1–8.
20. Drahos, L.; Peltz, C.; Vekey, K. Accuracy of Enthalpy and Entropy Determination Using the Kinetic Method: Are We Approaching a Consensus? *J. Mass Spectrom.* **2004,** *39,* 1016–1024.
21. Johnson, J. A.; Deppmeir, B. J.; Driessen, A. J.; Hehre, W. J.; Klunzinger, P. B.; Pham, I. N.; Wantanabe, M. *Spartan '02, 1.0.8*; Wavefunction: Irvine, CA, 2002.
22. Frisch, M. J.; Trucks, G. W.; Schlegel, H. B.; Scuseria, G. E.; Robb, M. A.; Cheeseman, J. R.; J. A. Montgomery, J.; Vreven, T.; Kudin, K. N.; Burant, J. C.; Millam, J. M.; Iyengar, S. S.; Tomasi, J.; Barone, V.; Mennucci, B.; Cossi, M.; Scalmani, G.; Rega, N.; Petersson, G. A.; Nakatsuji, H.; Hada, M.; Ehara, M.; Toyota, K.; Fukuda, R.; Hasegawa, J.; Ishida, M.; Nakajima, T.; Honda, Y.; Kitao, O.; Nakai, H.; Klene, M.; Li, X.; Knox, J. E.; Hratchian, H. P.; Cross, J. B.; Adamo, C.; Jaramillo, J.; Gomperts, R.; Stratmann, R. E.; Yazyev, O.; Austin, A. J.; Cammi, R.; Pomelli, C.; Ochterski, J. W.; Ayala, P. Y.; Morokuma, K.; Voth, G. A.; Salvador, P.; Dannenberg, J. J.; Zakrzewski, V. G.; Dapprich, S.; Daniels, A. D.; Strain, M. C.; Farkas, O.; Malick, D. K.; Rabuck, A. D.; Raghavachari, K.; Foresman, J. B.; Ortiz, J. V.; Cui, Q.; Baboul, A. G.; Clifford, S.; Cioslowski, J.; Stefanov, B. B.; Liu, G.; Liashenko, A.; Piskorz, P.; Komaromi, I.; Martin, R. L.; Fox, D. J.; Keith, T.; Al-Laham, M. A.; Peng, C. Y.; Nanayakkara, A.; Challacombe, M.; P. M. W. Gill; Johnson, B.; Chen, W.; Wong, M. W.; Gonzalez, C.; Pople, J. A. *Gaussian 03, Revision B04*; Gaussian, Inc.: Pittsburgh, PA, 2003.
23. Kumar, M. R.; Prabhakar, S.; Nagaveni, V.; Vairamani, M. Estimation of Gas-Phase Acidities of a Series of Dicarboxylic Acids by the Kinetic Method. *Rapid Commun. Mass Spectrom.* **2005,** *19,* 1053–1057.
24. Bouchoux, G.; Djazi, F.; Gaillard, F.; Vierezet, D. Application of the Kinetic Method to Bifunctional Bases MIKE and CID-MIKE Test Cases. *Int. J. Mass Spectrom.* **2003,** *227,* 479–496.
25. Cao, J.; Aubry, C.; Holmes, J. L. Proton Affinities of Simple Amines; Entropies and Enthalpies of Activation and Their Effect on the Kinetic Method for Evaluating Proton Aaffinities. *J. Phys. Chem. A* **2000,** *104,* 10045–10052.
26. Wesdemiotis, C. Entropy Considerations in Kinetic Method Experiments. *J. Mass Spectrom.* **2004**, *39*.
27. Bartmess, J. E. Negative Ion Energetics Data. In *NIST Standard Reference Database Number 69*, Mallard, W. G.; Linstrom, P. J., Eds. National Institute of Standards and Technology: Gaithersburg MD, 2008; http://webbook.nist.gov.